

THE PULMONARY RESPONSE TO HEMORRHAGIC SHOCK (U)
ANNUAL PROGRESS REPORT

by

Responsible Investigator: Richard H. Egdahl, M.D.

Co-Investigator: Herbert B. Hechtman, M.D.

31 July 1970

Supported by

U. S. ARMY MEDICAL RESEARCH AND DEVELOPMENT COMMAND
Washington, D. C. 20315

Contract No. DADA 17-68-C-8132

Boston University School of Medicine
Boston, Massachusetts 02118

This document has been approved for public release and sale; its distribution is unlimited.

The findings in this report are not to be construed as an official Department of the Army position unless so designated by other authorized documents.

Reproduced by the
CLEARINGHOUSE
for Federal Scientific & Technical
Information Springfield Va. 22151

AD 704 696

ABSTRACT

1. Institution: Boston University School of Medicine
80 East Concord Street
Boston, Massachusetts 02118
2. Title: The Pulmonary Response to Hemorrhagic Shock
3. Responsible Investigator: Richard H. Egdahl, M.D.
4. Co-Investigator: Herbert E. Hechtman, M.D.
5. Number of Pages: July 31, 1970
Date:
6. Contract Number: DADA 17-60-C-8132
7. Supported by: U. S. Army Medical Research & Development
Command, Department of the Army,
Washington, D. C. 20315

Indicator dilution methodology has been applied to the study of pulmonary hemodynamics and ventilatory function before and after hemorrhagic shock and in in-vitro perfused lungs. New sampling techniques have been developed and new mathematical models applied to data analysis.

Both vascular distention and the recruitment of new flow channels may play important roles in adaptive changes of the normal lung to varying cardiac outputs. After shock, pulmonary edema or prolonged in-vitro perfusion, pulmonary artery pressure rises and there is derecruitment. Other factors found to be of significance in the distribution of pulmonary flow and pulmonary function include posture, oxygen breathing and the pharmacologic agents norepinephrine, serotonin, endotoxin, dibenzylamine and acetylcholine.

A new method is described for the measurement of alveolar gas volumes and capillary blood volume.

KEY WORDS: HEMORRHAGIC SHOCK - PULMONARY EDEMA - DISTENTION - RECRUITMENT - INDICATOR DILUTION - PULMONARY FUNCTION

CONTENTS

1. Early Pulmonary Hemodynamic and Ventilatory Changes which Accompany Hemorrhagic Shock and <u>In-vitro</u> Pump Perfusion	
a) Normal Factors Controlling Distribution of Blood in the Pulmonary Microcirculation	1
b) Alterations in Distribution and their Association with Changes in Vascular Resistance	7
Pharmacologically Induced Changes in Capillary Flow and Alveolar Function	
c) Effects of Hemorrhagic Shock and Pulmonary Edema	11
d) Venous Admixture	12
2. Development of Mechanical Methods and Techniques.	
a) <u>In-vitro</u> Perfusion System	15
b) Mercury Injection Sampling System	16
c) Automated Data Collection and Analysis	16
3. New Approaches for the Measurement of Certain Indices of Pulmonary Function	
a) Alveolar Volume, Alveolar Ventilation	18
b) Capillary Blood Volume, Extra Vascular Volume	21
c) Venous Admixture	22

1. EARLY PULMONARY HEMODYNAMIC AND VENTILATORY CHANGES WHICH ACCOMPANY HEMORRHAGIC SHOCK AND IN-VITRO PUMP PERFUSION

a) Factors with Determine the Distribution of Blood in the Normal Lung

(1) Cardiac Output

A simple demonstration of the dependence of blood volume and flow is shown by the study in Fig. 1. A small tracer dose of Cr-51 labelled red cells was added to the in-vitro blood reservoir (Fig. 12) and allowed to equilibrate with the whole system. An external probe measured the radioactivity which directly reflected blood volume. As flow was increased there was little change in arterial pressure, indicating an increase in the cross-sectional area of the vascular bed. The added vascular volume must be due either to distention of vessels or to a recruitment of new parallel flow channels.

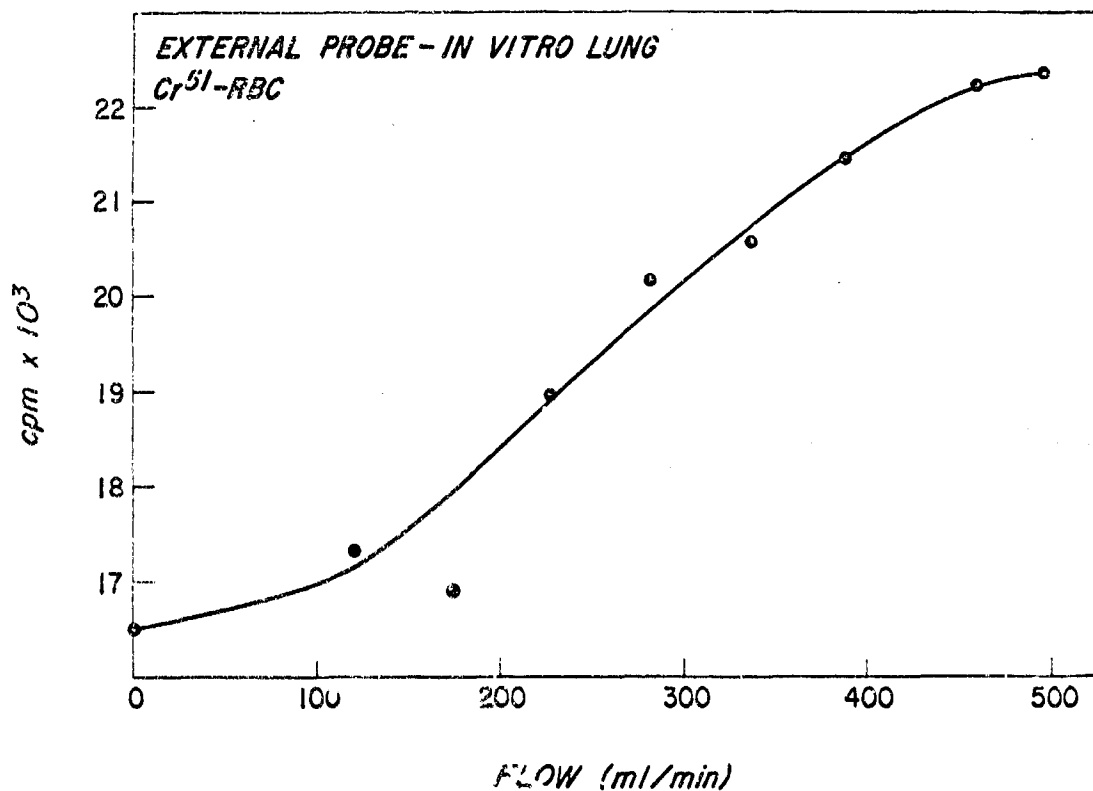


Fig. 1: Dependence of flow and pulmonary blood volume.

A single tracer (cardio-green dye or chromated red cells) indicator dilution technique provides similar data (Fig. 2). These experiments were done to verify the accuracy of the method. We found that indicator dilution flows agreed within 8% of the volumetrically determined flows.

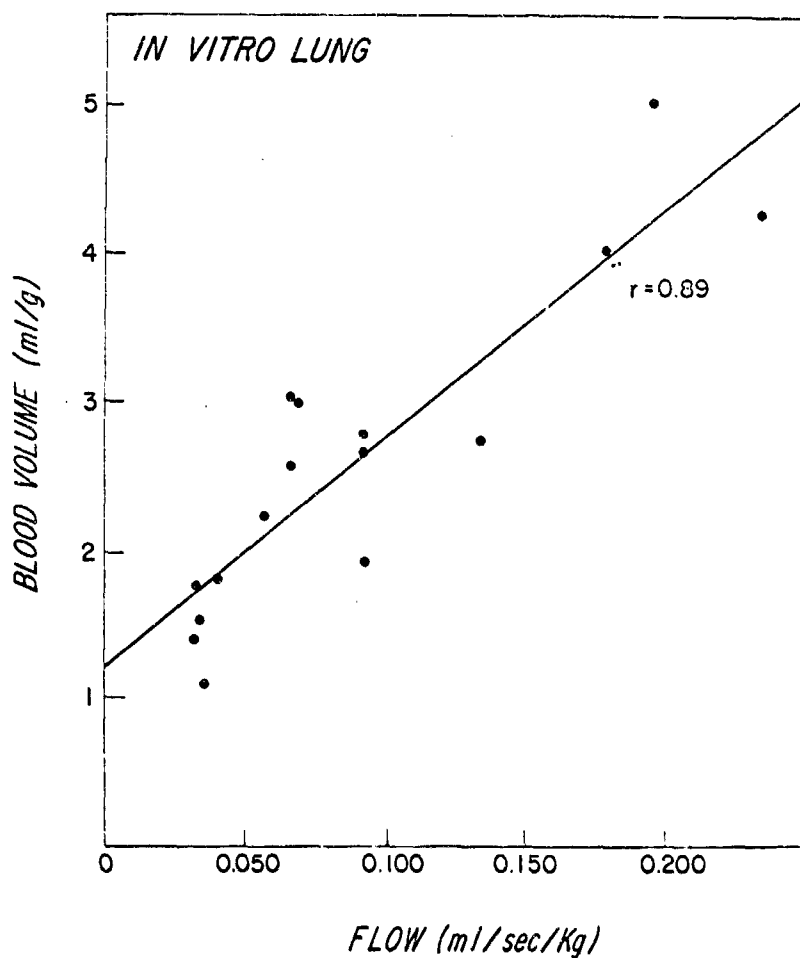


Fig. 2: Indicator dilution studies of the dependence of flow and volume. The tracers used were cardio-green or chromated red cells. Each dot represents a separate lung.

We then examined the flow and central blood volume in a series of normal dogs and compared them to another series subjected to hemorrhagic shock (Fig. 3). Again we found a good correlation of flow and volume. Injection into the right atrium via the jugular vein gave us the additional volume of the right heart. Dogs subjected to hemorrhagic shock showed no significant volume changes from controls.

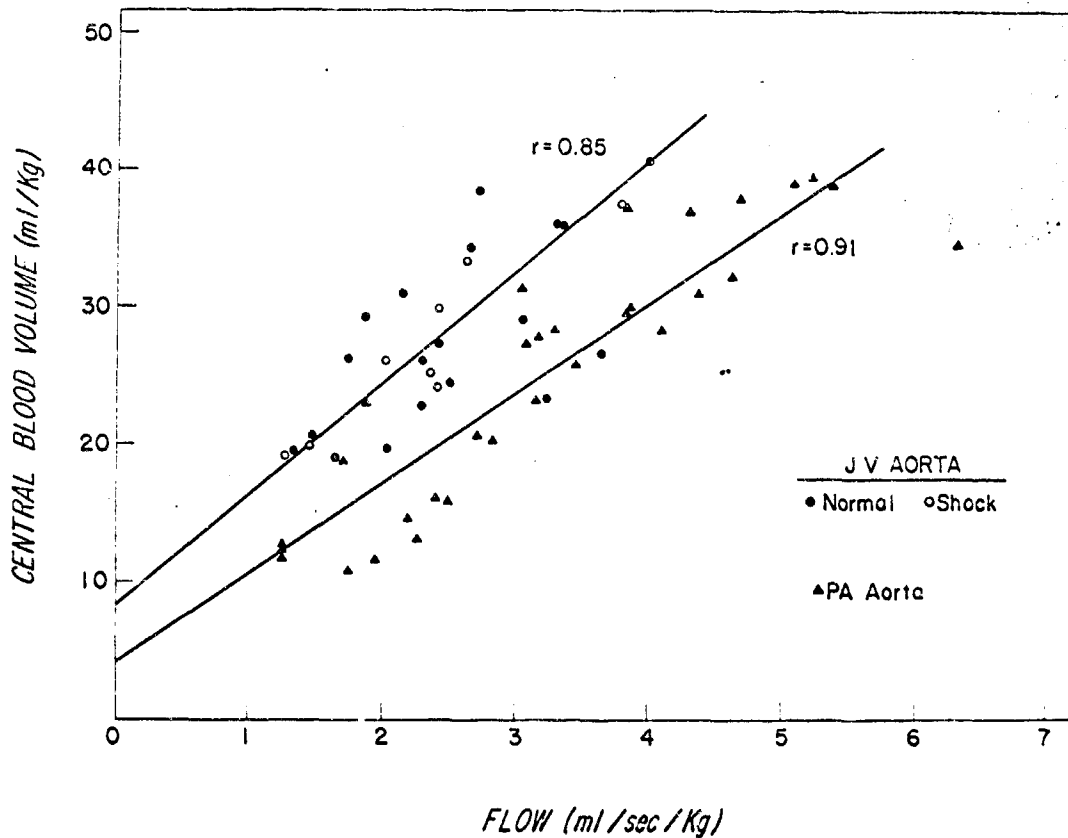


Fig. 3: The central blood volume after hemorrhagic shock did not differ significantly from normal controls.

The question of vascular recruitment vs. distensibility was next examined with the use of a multiple indicator dilution method (1) (Fig. 4). A series of in-vitro perfused lungs were studied prior to the onset of pulmonary edema using cardio-green, I-131 antipyrine and xenon-133.

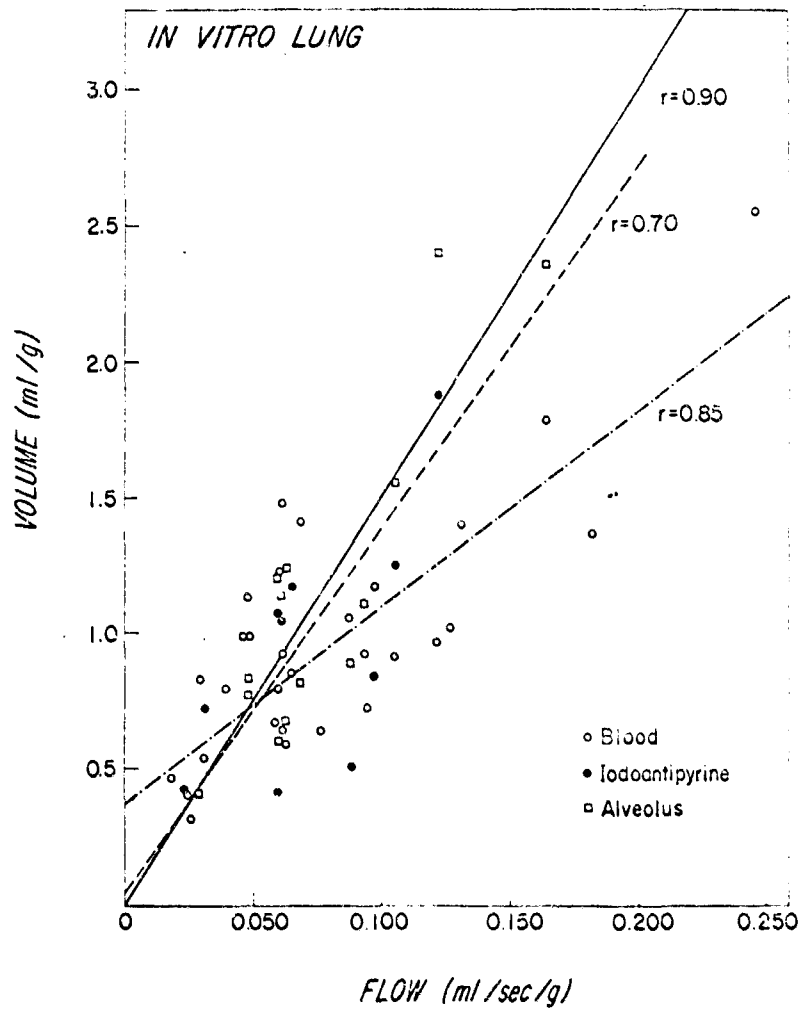


Fig. 4: Indicator dilution measurements of blood volume, water volume and alveolar air volume (see text). This represents results from ten different lungs.

As pulmonary flow increased the central blood volume, water volume and effective alveolar air volume (EAAV) increased. The latter two measurements are based on indicator dilution methodology (see section 3a) and therefore relate only to those volumes which surround perfused capillaries. Thus with changes in flow there are changes in the number of perfused capillaries, a phenomena which we describe as recruitment. An increase in vascular volume with no change in water volume is interpreted as distention. The slope of the vascular volume is less steep than the antipyrine volume (considered to measure the water space) or the EAAV. This is probably related to the large base line volume of blood in the arteries and veins which tends to dampen the effect of added increments of capillary blood volume.

(2) Gravity

Previous work by others has repeatedly demonstrated the importance of position in determining regional blood flow. We studied this phenomenon in dogs by alternate positioning of the animal in the left and right lateral decubitus position (Fig. 5).

In the normal dog, the decrease in flow in going from the left to right lateral decubitus position readily explains the decrease in blood volume and effective alveolar air volume (EAAV). The latter represents the volume of air in alveoli that are perfused. Alveolar ventilation also decreases. These findings are consistent with a decrease in the perfusion of capillary alveolar units secondary to a decrease in flow. The postural effect is seen in the significant increase in venous admixture $\left(\frac{QS}{QT}\right)$. This type of evidence indicates that not only may there be a quantitative change in the number of capillary alveolar units being perfused but that there may also be a quantitative change in pulmonary function depending on the redistribution of flow. In another study (Fig. 5), venous admixture almost doubled when the experimental animal was turned onto his right side. The V/Q ratio decreased from .706 to .306. Post mortem examination showed severe pneumonia primarily affecting the right lung. A similar change was noted in a study one hour after shock where turning resulted in a diminution of venous admixture and an increase in the V/Q ratio from .796 to 1.042. The changes in EAAV in these stressed animals was not consistent with recruitment due to altered flow. The changes argue for a redistribution of flow based on gravitational effects to lung regions with different functional capacities.

POSTURE & PULMONARY FUNCTION

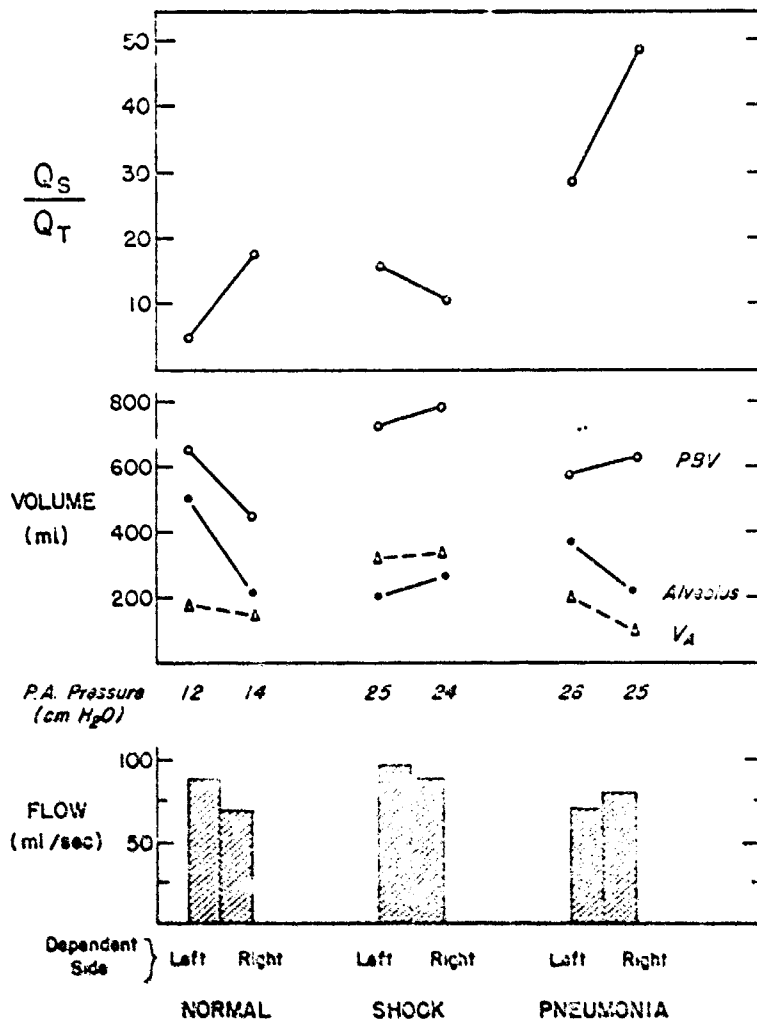


Fig. 5: Positional effects on the distribution of blood flow and pulmonary function.

b) Pathological and Physiological Alterations in the Distribution of Flow - Relationship to Pulmonary Arterial Pressure

(1) The normal lung handles increases in flow with recruitment of new vascular channels and/or distention of existing channels. Pulmonary pressure is therefore relatively unaffected with large flow changes. Either phenomena may be operative and may be effective in preventing pressure changes. Fig. 6 demonstrates a relatively stable EAAV despite a very large increase in blood volume with increasing flow. Pulmonary artery pressure rose but slightly because of this vascular distention.

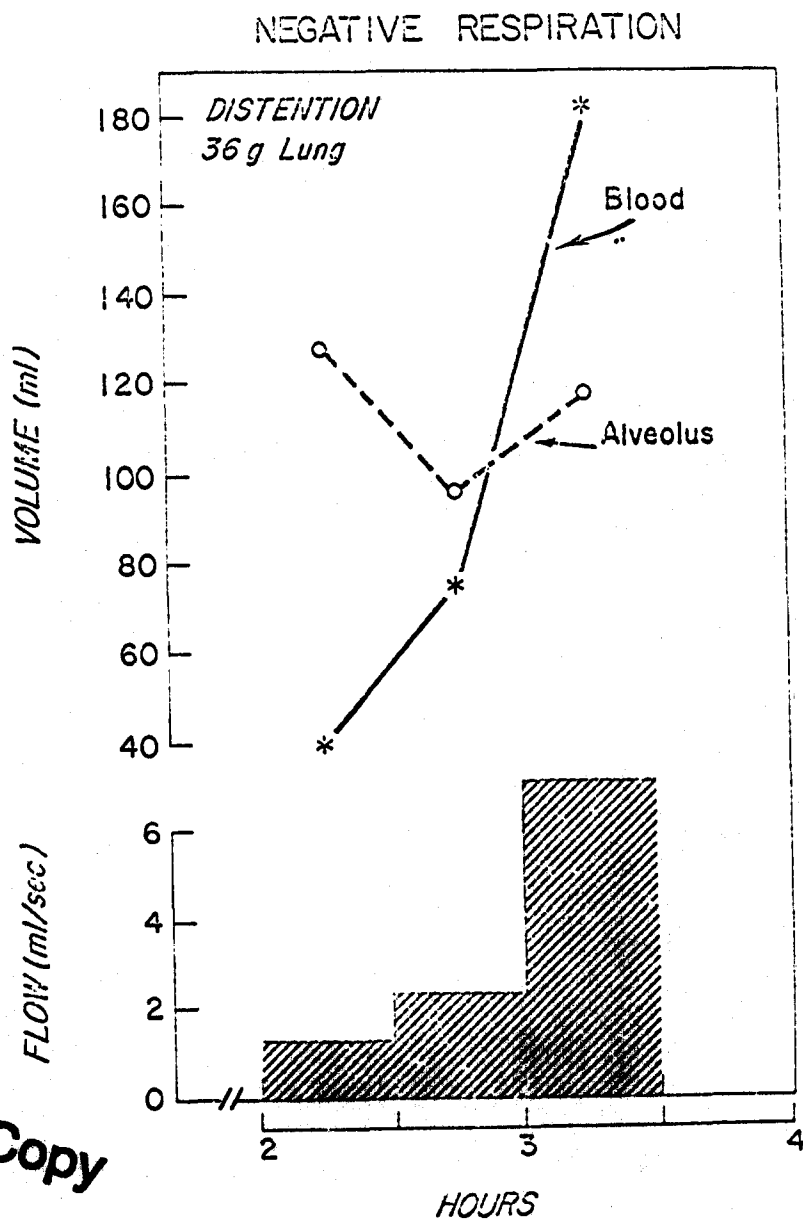


Fig. 6: The large step increases in flow were accompanied by the slight increases in pulmonary artery pressure.

Best Available Copy

Recruitment as a protective mechanism is demonstrated in Fig. 7. Here blood volume is stable while antipyrine and water volumes vary directly with flow.

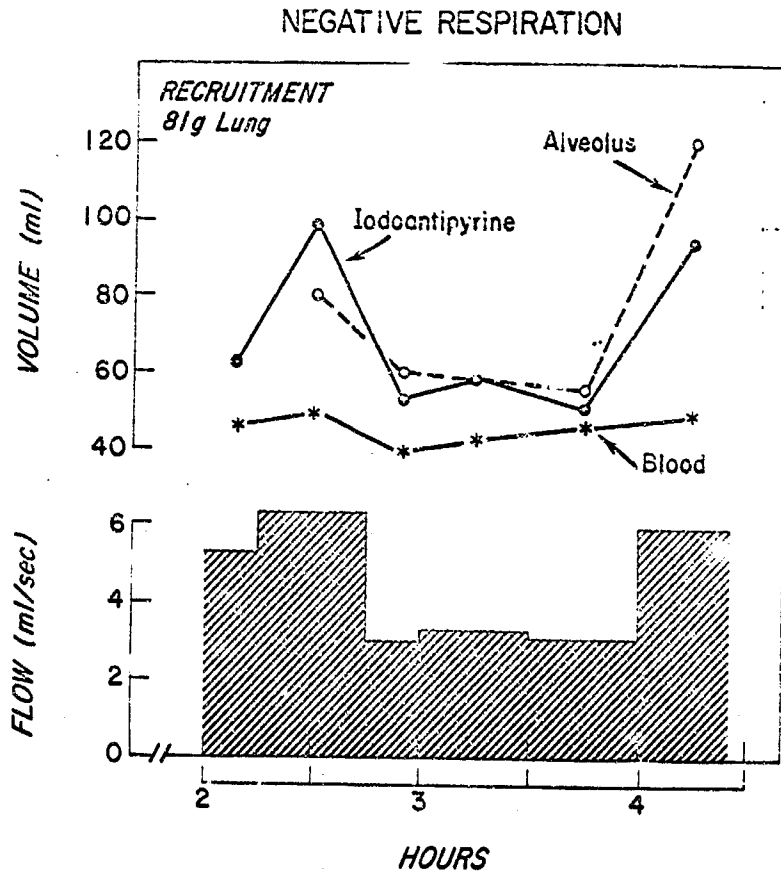


Fig. 7: Alveolar and antipyrine volumes follow flow indicating changes in the number of functioning alveolar-capillary units.

(2) Pulmonary edema was studied in-vitro. Its occurrence was usually accompanied by an increase in vascular resistance. Fig. 8 shows derecruitment and vascular distention accompanying the progression of pulmonary edema whereas Fig. 9 illustrates partial pharmacological reversal, with both recruitment and a diminution of mean pulmonary artery pressure from 38 to 30 cm H₂O when dibenzylene was given.

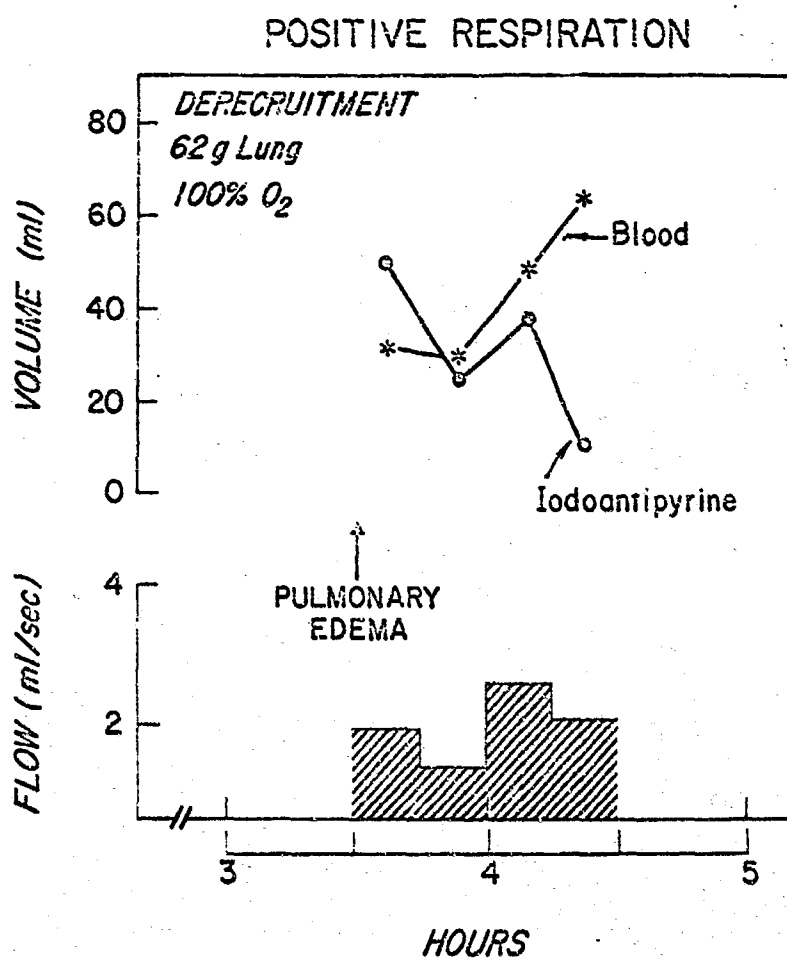


Fig. 8: Pulmonary edema is associated with increase in pulmonary arterial pressure, distention of blood vessels (increase in blood volume) and derecruitment of capillary channels (decrease in measured water).

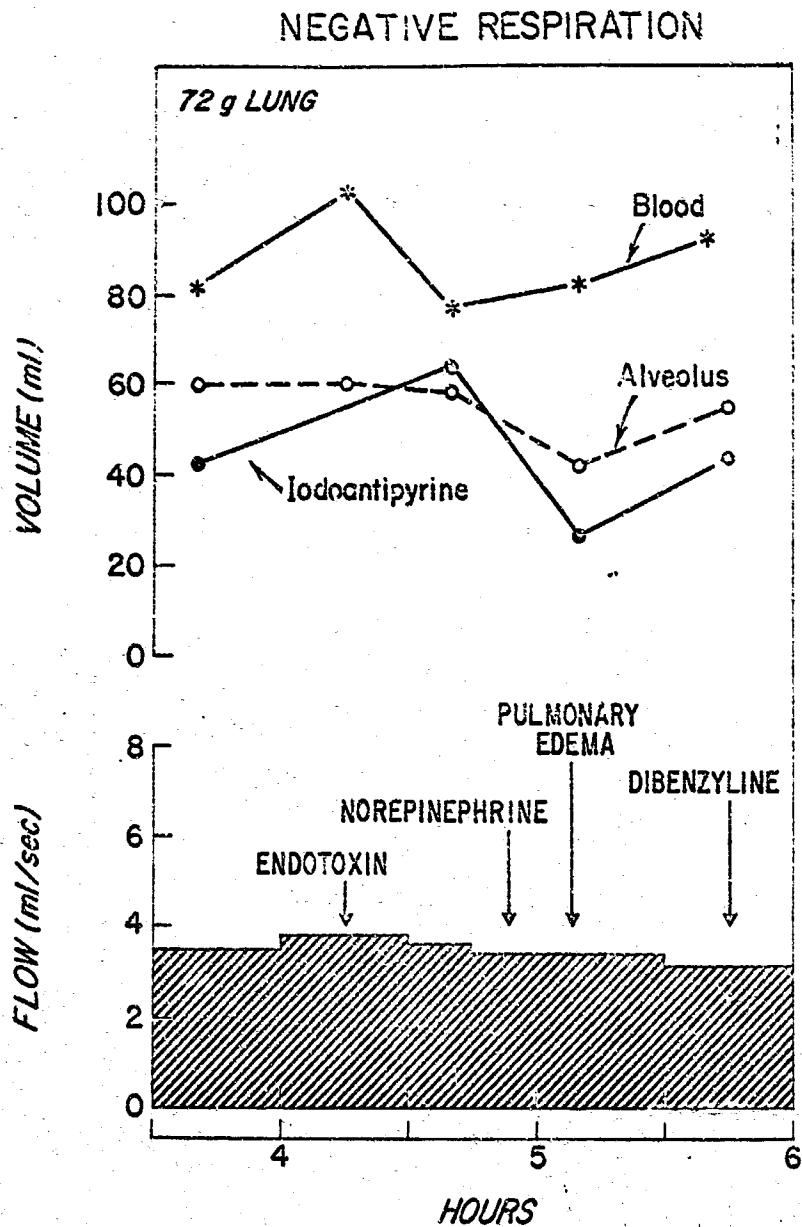


Fig. 9: Partial pharmacologic reversal of the closing of alveolar-capillary units with dibenzylene.

(3) We have preliminary data concerning various pharmacologic agents.

Dibenzylena is consistent in its ability to increase vascular recruitment.

Serotonin raises pulmonary artery pressure, while paradoxically increasing recruitment. This increase in resistance is due to vascular constriction since the pulmonary blood volume is decreased.

Acetylcholine in the dosage used, produced no changes in pulmonary artery pressure but produced a dramatic decrease in the number of perfused capillaries while causing vascular distention.

Endotoxin and norepinephrine had similar effects which were the reverse of acetylcholine. A rise in vascular resistance was noted.

Isoproterenol reversed the effects of serotonin with regard to recruitment. Its effects in the normal lung are not yet clear.

c) Effects of Hemorrhagic Shock and Pulmonary Edema (2)

After prolonged pump perfusion the gross changes of patchy "congestive atelectasis" were seen. These are areas of the lung which collapse completely on expiration but re-expand at least partially on inspiration. Pulmonary edema, with bronchial froth, appeared later. Neither of these events was associated with an increase in venous admixture. This surprising observation is explained by our findings of progressive derecruitment. It appears as if the damaged segments of the lung were no longer perfused. Thus, the measured lung water may continue to decrease despite a progressive increase in lung weight. Such findings should caution against the simple use of a two-tracer technique for the measure of total lung water, particularly with pulmonary disease and increase in vascular resistance.

The effective alveolar air volume (EAAV) falls progressively after prolonged pump perfusion. EAAV was also measured one hour after hemorrhagic shock (Table 1) and was found to have decreased significantly ($p < .01$). In the animals that survived one day, the volume returned toward normal. The first seven dogs were studied while breathing while the last four dogs were studied during breath holding. The latter volumes are larger because of the inclusion of dead space with this measurement technique. Two control animals showed no change after 8-10 hours of anesthesia.

ALVEOLAR GAS VOLUMES

Before Shock	One Hour After Shock	One Day After Shock
15.8	6.3	12.3
8.9	5.3	8.3
11.1	8.9	
7.3	3.0	
13.3	9.7	6.6
18.2	7.4	18.3
7.8	6.8	
37.9	24.9	
21.6	12.3	
45.3	35.1	22.3
23.9	26.5	33.2

Table 1: Alveolar air volumes after hemorrhagic shock.

We are not yet certain whether this decrease in alveolar air represents simply derecruitment or whether interstitial edema and possible loss of surfactant also encourage alveolar collapse. This latter possibility is suggested by frequent decreases in surface activity that we see in the in-vitro lungs as measured by the Pattle bubble stability technique.

d) Venous Admixture

The breathing of 100% oxygen is a technique used to calculate anatomic shunting using the Berengren assumption. The technique requires a twenty minute period of 100% O₂ breathing before one can be reasonable certain that all N₂ is washed out of poorly ventilated alveoli. We have noted that during this time period the amount of gross atelectasis may increase. This phenomena is described by others and is a known hazard of O₂ breathing. We have observed that cardiac output decreases during 100% oxygen breathing. Alveolar ventilation and effective alveolar volume also change. We do not believe, therefore, that steady state conditions exist after the shift from room air to 100% oxygen breathing, to justify the use of this technique to differentiate the various forms of venous admixture.

We examined the use of the inert gases, xenon-133 and later krypton-85, as an approach to the measure of venous admixture. The model we formulated is diagramed in Fig. 10 which is a schematic of a capillary alveolar unit.

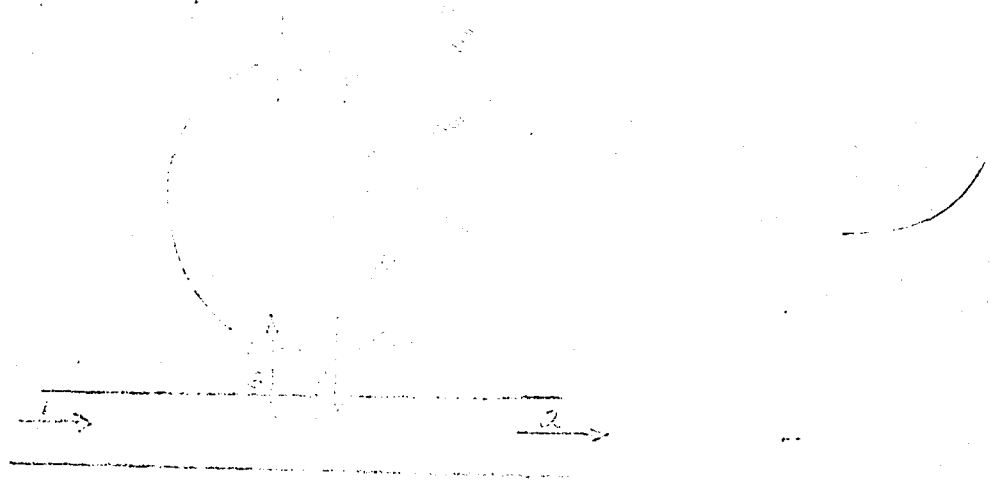


Fig. 10: Model of gas exchange in a capillary alveolar unit: 1 and 2 are blood input and exit, 3 and 4 are equilibrium across the interstitial space; 5 and 6 represent bulk air movement as well as diffusion.

In the breathing state, we found a direct correlation between alveolar ventilation ($\uparrow V_A$ and $\downarrow \dot{V}$) and the vascular recovery of xenon. Secondly, we have observed that if V_A is kept constant, xenon recovery becomes a direct function of flow. In breath holding (resting lung volume) we recover an average of only 60% of the injected xenon (Fig. 11). The only pathway for loss is diffusion ($\uparrow \dot{V}$). If we induce atelectasis there is a 95% recovery since diffusion loss is minimized. The scatter of data in the breathing lung in Fig. 11 is therefore explained by the dependence of xenon recovery not only on the shunt Q_S/Q_T but also on V_A , flow and diffusion. If $Q_S/Q_T = 0$, xenon recovery is about 10%. If the pulmonary shunt is due to true atelectasis, there will be virtually complete vascular recovery of our gas tracer through the area. In non-ventilated areas recoveries of 45-75% are expected. If some ventilation occurs this recovery will decrease to very low levels.

We therefore draw the following conclusions from this data.

- (1) If $\frac{X_e^*}{CG} > \frac{Q_S}{Q_T}$ by more than 10% this signifies primarily atelectasis or true precapillary shunting.
- (2) If $\frac{X_e}{CG} = 45-75\% \frac{Q_S}{Q_T}$ this signifies a shunt through areas containing air, but which are not ventilated.
- (3) If $\frac{X_e}{CG} < 45\% \frac{Q_S}{Q_T}$ we are dealing with air containing, poorly ventilated alveoli.

$\frac{X_e^*}{CG}$ recovery of xenon related to the internal standard cardio-green.

These distinctions may be of practical clinical significance. After hemorrhagic shock, the data in Fig. 11 indicates atelectasis is not the usual cause of shunting.

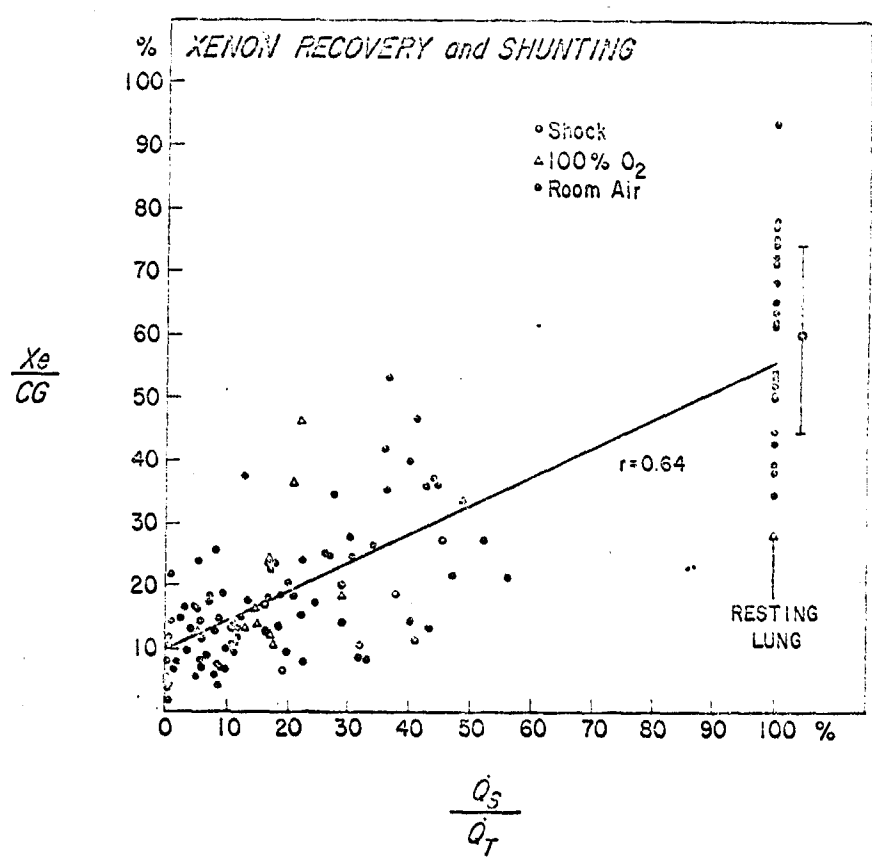


Fig. 11: Xenon recovery is a function not only of the "pulmonary shunt $\frac{Q_s}{Q_T}$, but also V_A , cardiac output and diffusion.

In 100% O₂ breathing (a measure of "anatomic shunt") Xe recovery was greater than $\frac{Q_s}{Q_T}$ in 14 out of 15 in-vitro experiments.

Early data concerning 100% O₂ breathing is shown in Fig. 11. The studies were done in animal and is not consistent with our in-vitro experience. We believe this may be due to failure of delivery of 100% O₂, since our system was not leak proof.

2. DEVELOPMENT OF MECHANICAL METHODS AND TECHNIQUES

a) In-vitro Perfusion System (Fig. 12)

A system is currently in use which provides control of flow, arterial and venous pressure, pleural pressure, temperature, humidity and gas content of the pulmonary artery blood. We are currently building a pulsatile pumping system and we plan to mount a force-displacement transducer within the inner box for monitoring lung weight changes.

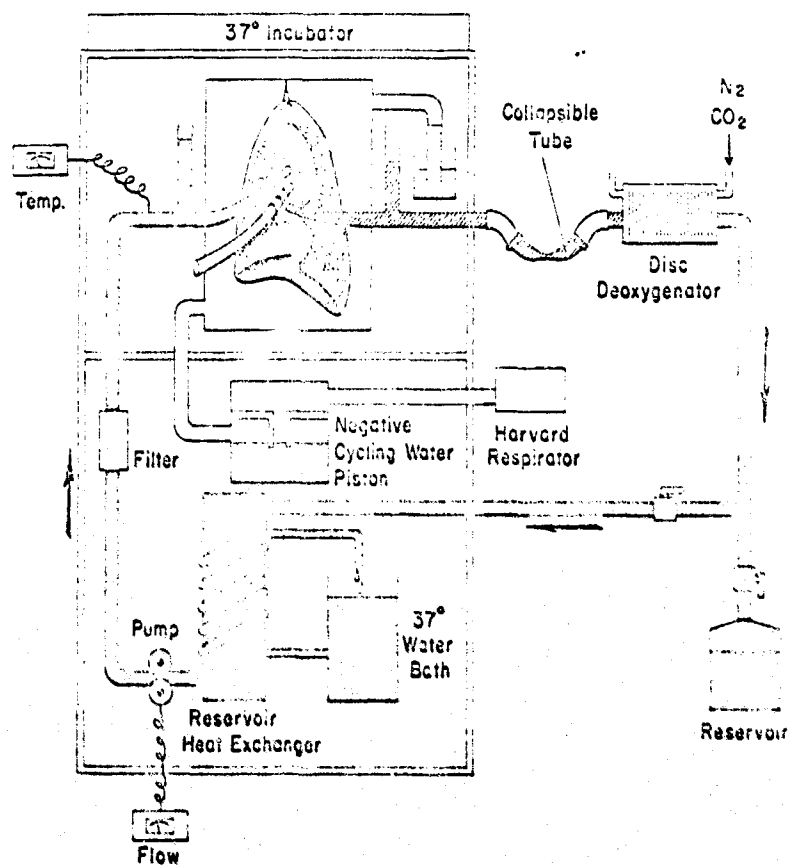


Fig. 12: In-vitro perfusion system. Flow, pressures, temperature, humidity and blood gases are controlled.

b) A mercury injection system (Fig. 15) is fully tested and has proven invaluable for the rapid accurate counting of blood (5). It is now fitted with a magnetic sensor to detect the droplets of mercury, and circuitry has been designed and built to allow completely automated counting of an entire run.

c) A tape system has been integrated with our detector and a channel scaler to record the indicator dilution runs. A plotter has been evolved which permits the IBM 1401 to draw the indicator curve as well as extrapolate, calculate areas and mean transit time.

MERCURY INJECTION SAMPLING SYSTEM

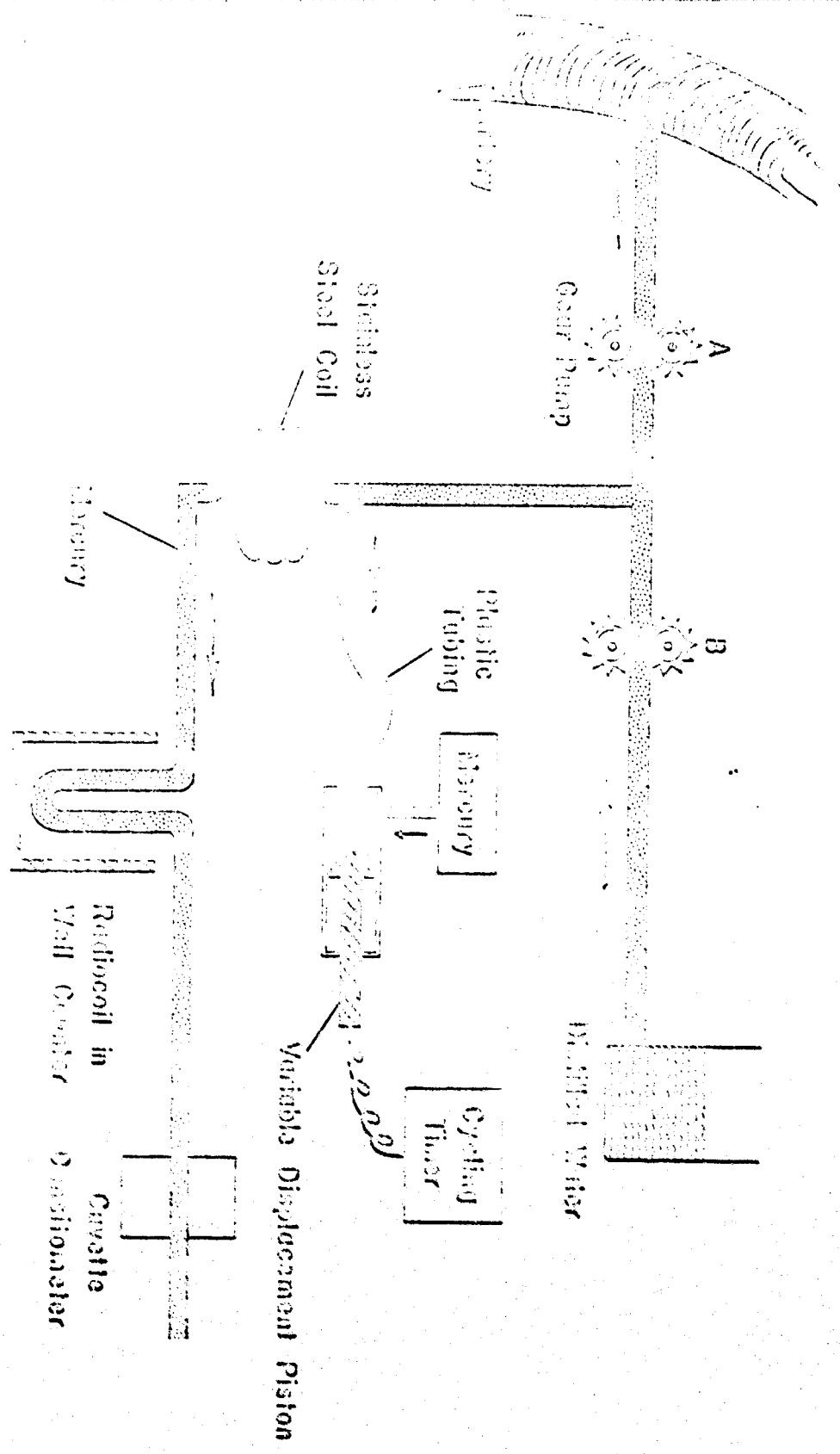


Fig. 13: Components of the Mercury Injection Sampling System. Additional stainless steel coils may be coupled in parallel for sequential runs.

2. ALVEOLAR VOLUME, ALVEOLAR VENTILATION

a) Alveolar Volume, Alveolar Ventilation

After injection of xenon into the pulmonary artery in a breathing lung, xenon clearance is determined by alveolar ventilation, alveolar volume and blood flow. We have found that ventilation is the most significant factor. Indeed, if we inject the two inert gases xenon-133 and krypton-85 we find the mean transit times of their indicator dilution curves are equal (15 experiments) and that their recoveries in blood are related to their Ostwald solubility coefficients ($\frac{t'_{Xe}}{t'_{Kr}} = \frac{S_{Xe}}{S_{Kr}} = 1.7$).

Thus the gases exit the alveolus via air channels at a rapid and equal rate maintaining equal concentrations in the alveolus. Their uptake by blood (recovery) is a function of their solubilities. In order to convert the transit time (t'_{Xe}) we divide it by the blood uptake (recovery).

$$1 \quad t'_{Xe} = \frac{\bar{t}_{Xe}}{\text{Fraction Xe recovered}}$$

2 Total volume of gas in alveoli during the indicator dilution run (V) = resting alveolar volume + (no. respiratory cycles during the time interval \bar{t}_{Xe} - cardiac-growth) (alveolar ventilation per breath)

3 $V = \text{Flow} (t'_{Xe} - \bar{t}_{\text{cardio-growth}}) (Ostwald solubility coefficient xenon)$

This total volume (V) is measured experimentally. We also know:

4 Ventilatory clearance = 1 - recovery of xenon in blood

A graphical solution is most convenient to calculate ventilatory clearance/cycle.

5 Ventilatory clearance per cycle = $\frac{\text{Alveolar ventilation}}{\text{Resting alveolar volume} + \text{ventilation}}$

The two unknowns: alveolar volume and alveolar ventilation are then solved algebraically from equations 2 and 5.

Experimental work has been done to verify this technique. Values show each obtained by blood sampling and simultaneous external flow monitoring. Clearance calculated by the more standard external flow data agrees precisely with the indicator dilution data. (Values were

the xenon indicator dilution curve should be moved to the right four seconds). Most important, alveolar ventilation calculated from mixed expired CO_2 and arterial CO_2 is in good agreement with alveolar ventilation calculated by the xenon methods. Four other experiments also show good correlation. The CO_2 method always gives slightly higher results. We believe this is due to rebreathing of dead space and therefore measurement of an abnormally high mixed expired CO_2 .

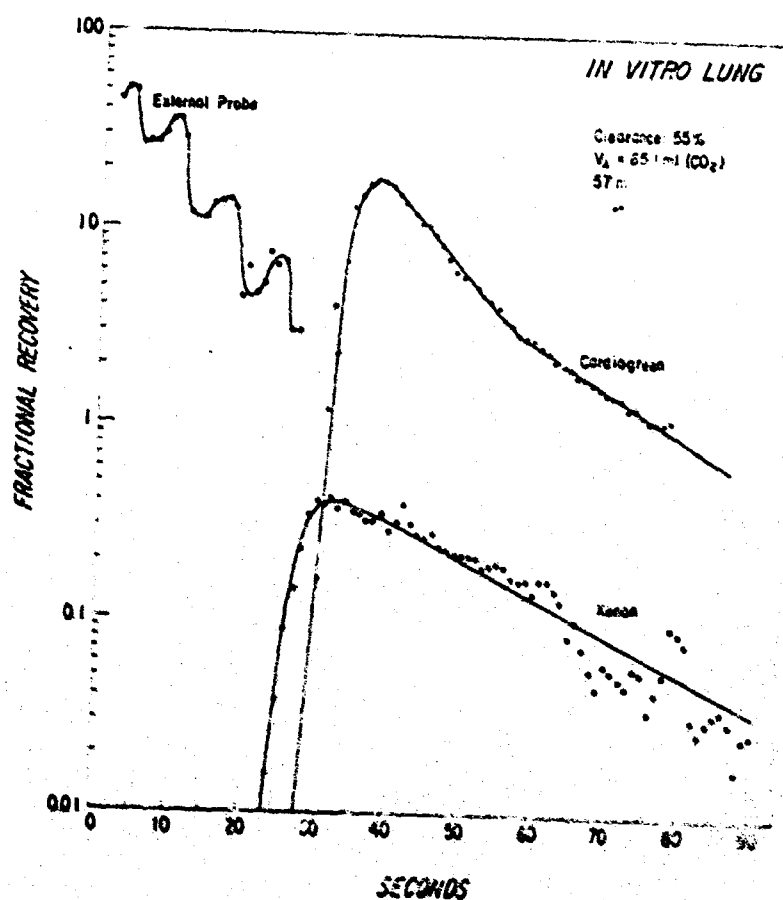


Fig. 14: Agreement of xenon clearance values calculated from the external probe and indicator dilution data. Alveolar ventilation derived from mixed expired CO_2 and arterial pCO_2 tension is some what higher than alveolar ventilation obtained from the indicator dilution curves.

The relationship of xenon recovery to V_A and flow is shown in Fig. 15.

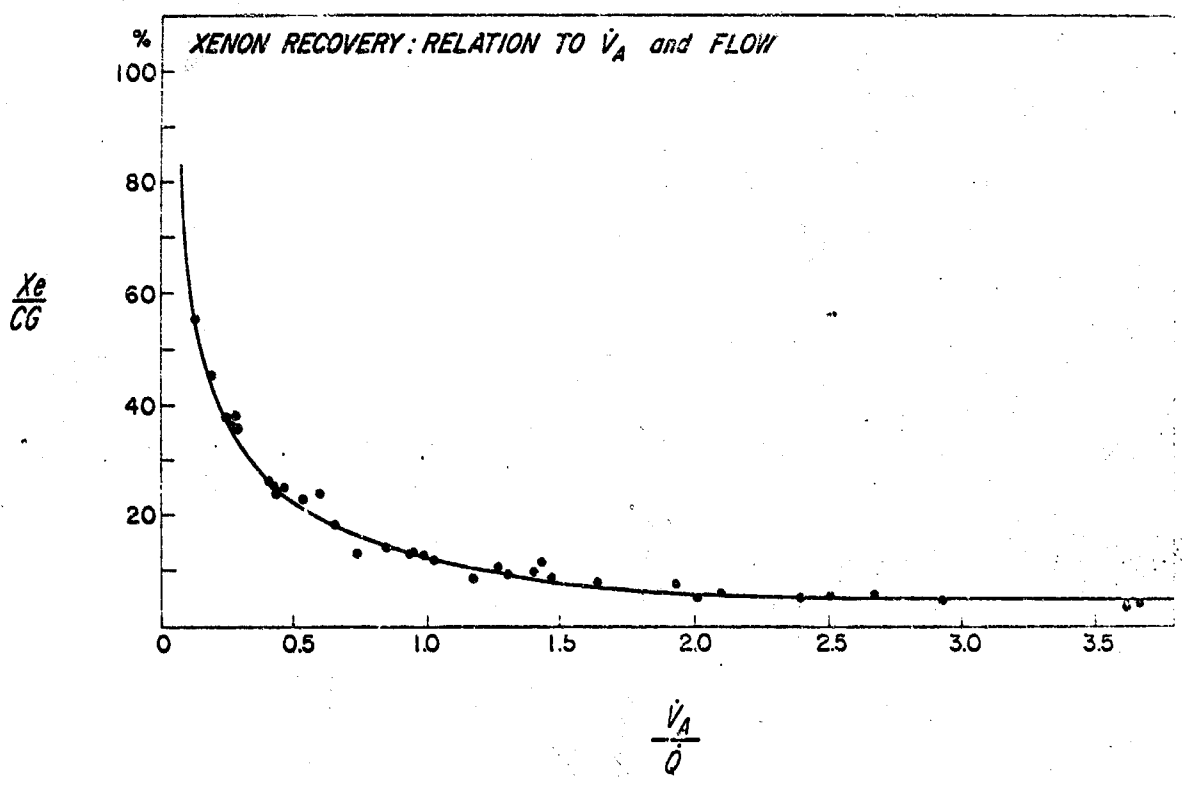


Fig. 15

b) A New Approach for the Simultaneous Determination of Capillary Volume (V), Extravascular Volume (V') and Alveolar Gas Volume (V)

We have observed that the gases xenon-133 or krypton-85 appear a fraction of a second earlier than a simultaneously injected vascular label such as cardio-green dye or chromated red cells. In order to analyze this data a simple model describing arterial, capillary and venous blood flow was developed (Fig. 15). In this figure, the pre-capillary, capillary and post capillary blood is represented by the sections a to b, b to c and c to d respectively. The capillary blood volume is v , the lung tissue volume is v' and the alveolar volume is V . The terms h_1 , h_2 and h_3 are the "transfer functions" describing, for h_1 for example, the tracer concentration occurring at b following an impulse of tracer applied at point a. The transfer function for the entire system from a to d is just the convolution of the three inter-current transfer functions, that is $h_1 \otimes h_2 \otimes h_3$. Convolution is a mathematical type of "multiplication" which is used to relate transfer functions to one another in the time domain; it is analogous to multiplying the Laplace transforms of transfer functions in the frequency domain.

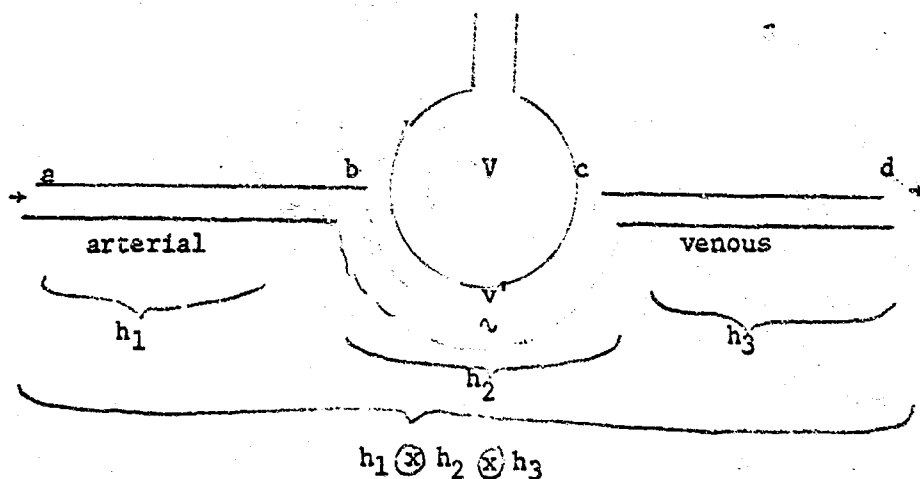


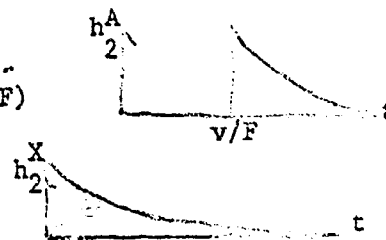
Fig. 16: A model describing flow and volumes in a capillary-alveolar unit.

Three tracers are used: cardio-green (G), antipyrine (A) and xenon (X). It is assumed that cardio-green has a purely vascular distribution, antipyrine and xenon both have tissue and vascular distributions. Xenon has in addition an alveolar distribution. The experiments to be analyzed were performed by the simultaneous injection of impulses (boluses) of the tracers at point "a." The time history of tracer concentrations at point "d" were measured. This information coupled with the modeled form of h_2 for each of the tracers will provide information about the anatomy of the section b-c and the alveoli.

The following simple forms of h_2 for each of the tracers listed above are proposed as an initial trial for identifying capillary volume, alveolar volume and lung tissue volume. The following assumptions are made: $h_1^A = h_1^X$, $h_3^A = h_3^X$, F = blood flow (constant), xenon equilibrates between b and c through the alveoli much more rapidly than blood flow from b- to c. Using the partition coefficient for xenon and antipyrine, the following simple models for the transfer functions h_2 for each of the three tracers proposed are defined:

$$\text{antipyrine: } h_2^A(t) = \frac{F}{.7v' + v} e^{-\frac{F}{.7v' + v} (t - \frac{v}{F})} \mu^{-1}(t - v/F)$$

$$\text{xenon: } h_2^X(t) = \frac{Ft}{5V + v} e^{-\frac{Ft}{5V + v}} \mu^{-1}(t)$$



Following the injection of the three tracers at point a and their measurement at point d to determine the overall transfer function $h_1 \otimes h_2 \otimes h_3$ the following error function can be defined:

$$h_1^A \otimes h_2^A \otimes h_3^A \otimes h_2^X - h_1^X \otimes h_2^X \otimes h_3^X \otimes h_2^A = e_1(v, V, v', F)$$

The function $e_1(v, V, v', F)$ can now be minimized with fairly standard techniques to produce the optimum values of $F/(5V + v)$, $F/(.7v' + v)$ and v/F . The volumes of distribution of cardio-green and of antipyrine give the lung blood volume and total lung tissue volume respectively. All of this information may then be used to estimate v, V, v', F .

c) Venous Admixture

Three approaches are being taken to characterize the types of venous admixture.

(1) Transit Time Data of One Inert Gas

If a true precapillary shunt is present, an inert gas tracer will not evolve into an extravascular space. The transit time through this shunt will be relatively short compared with the mean transit time of a vascular tracer (fig. 17).

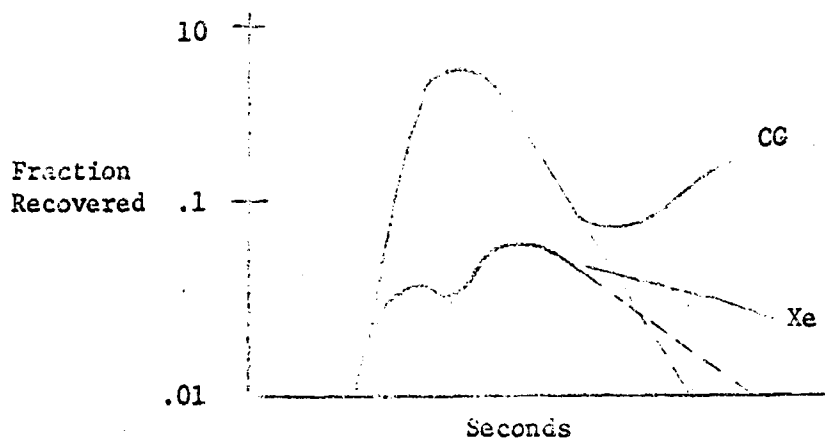


Fig. 17: The shaded area of the xenon curve represents a preferential vascular pathway.

(2) Double Gas Tracer Studies

Using 2 gases, xenon-133 and krypton-85, with different solubilities in blood and tissue, the possibility exists of describing types of venous admixture. We have preliminary data describing transit time and recovery data for these gases under various conditions.

(3) External Monitoring to Measure Regional Venous Admixture

The breath holding lung may be described as a two-compartment system with regard to the vascular washout pattern of xenon. The slow component represents air filled alveoli and disappears during breathing. This is strong evidence of functional significance of this two-compartment system. The fractional area of the rapid component equals $\frac{Q_s}{QT}$.

The same two-compartment system has been analyzed by graphical methods from the xenon curve drawn by external monitoring. In initial studies this has provided a method for the external detection of shunts.

BIBLIOGRAPHY

1. Hechtman, H. B., A. H. Herman, Indication dilution studies of lung function. Accepted by Society for Microcirculation.
2. Hechtman, H. B., A. H. Herman, B. C. Dorn, Pulmonary vascular, water and alveolar volumes in shock. Submitted to Surg. Forum.
3. Hechtman, H. B., R. E. Justice, A. H. Herman, A mercury injection system for the rapid anerobic sampling of blood. Accepted by the J. Appl. Physiol.

DOCUMENT CONTROL DATA - R 810

Security Classification: *Security classification, location of title, type of abstract and indexing classification must be entered when the overall report is classified.*

ORIGINATING AGENCY (Do not write authority) U. S. Army Medical Research and Development Command Department of the Army Washington, D.C. 20315	22. REPORT SECURITY CLASSIFICATION Unclassified <hr/> 23. GROUP Unclassified
--	---

24. REPORT TYPE

THE PULMONARY RESPONSE TO HEMORRHAGIC SHOCK

4. DESCRIPTIVE NOTES (Type of report and Inclusive dates)
 Annual Progress Report - 1 August 1969 - 31 July 1970

5. AUTHOR(S) (First name, middle initial, last name)
 Responsible Investigator: Richard H. Egdahl, M.D.
 Co-Investigator: Herbert B. Wechtman, M.D.

6. REPORT DATE 31 July 1970	79. TOTAL NO. OF PAGES 23	70. NO. OF REFS 3
8. CONTRACT OR GRANT NO. DADA 17-68-C-8132	82. ORIGINATOR'S REPORT NUMBER(S) 2	
9. PROJECT NO. . .	89. OTHER REPORT NO(S) (Any other numbers that may be assigned this report) 4689-5	

10. DISTRIBUTION STATEMENT
 This document has been approved for public release and sale; its distribution is unlimited.

11. SUPPLEMENTARY NOTES	12. SPONSORING MILITARY ACTIVITY Surgical Service U. S. Army Medical Research and Development Command, Washington, D.C.
-------------------------	---

13. ABSTRACT

- Indicator dilution methodology has been applied to the study of pulmonary hemodynamics and ventilatory function before and after hemorrhagic shock and in in-vitro perfused lungs. New sampling techniques have been developed and new mathematical models applied to data analysis. (U)

Both vascular distention and the recruitment of new flow channels may play important roles in adaptive changes of the normal lung to varying cardiac outputs. After shock, pulmonary edema or prolonged in-vitro perfusion, pulmonary artery pressure rises and there is derecruitment. Other factors found to be of significance in the distribution of pulmonary flow and pulmonary function include posture, oxygen breathing and the pharmacologic agents nor-epinephrine, serotonin, endotoxin, dibenzylamine and acetylcholine. (U)

A new method is described for the measurement of alveolar gas volumes and capillary blood volume. (U)

FORM 1470, 1 JAN 68, WHICH IS OBSOLETE FOR ARMY USE.

Security Classification

14. KEY WORDS	LINK A		LINK B		LINK C	
	ROLE	WT	ROLE	WT	ROLE	WT
Memorrhagic Shock						
Pulmonary Edema						
• Distention						
• Recruitment						
Indicator Dilution						
Pulmonary Function						